*Progress In Electromagnetics Research C, Vol. 79, 101–113, 2017*

# Gaussian Beam Electromagnetic Scattering from PEC Polygonal Cross-Section Cylinders

**Mario Lucido*, Fulvio Schettino, Marco D. Migliore, Daniele Pinchera, and Gaetano Panariello**

**Abstract**—In scattering experiments, incident fields are usually produced by aperture antennas or lasers. Nevertheless, incident plane waves are usually preferred to simplify theoretical analysis. The aim of this paper is the analysis of the electromagnetic scattering from a perfectly electrically conducting polygonal cross-section cylinder when a Gaussian beam impinges upon it. Assuming TM/TE incidence with respect to the cylinder axis, the problem is formulated as electric/magnetic field integral equation in the spectral domain, respectively. The Method of analytical preconditioning is applied in order to guarantee the convergence of the discretization scheme. Moreover, fast convergence is achieved in terms of both computation time and storage requirements by choosing expansion functions reconstructing the behaviour of the fields on the wedges with a closed-form spectral domain counterpart and by means of an analytical asymptotic acceleration technique.

## 1. INTRODUCTION

From a theoretical point of view, it is a normal practice to assume a plane wave as incident field in scattering problems. This simplification is justified by the basic idea that a general incident field can be represented in terms of continuous spectrum of plane waves. Following this line of reasoning, much effort has been devoted in the past years to the analysis of the scattering of a plane wave from perfectly electrically conducting (PEC) and dielectric objects. So, different techniques, such as method of moments [1], finite elements method [2], boundary elements method [3], the geometrical theory of diffraction and the uniform theory of diffraction [4, 5], and so on, have been proposed, depending on the complexity and the electrical size of the involved objects.

However, experimental results in scattering problems are in general obtained by means of incident fields produced by a radar antenna or a lens collimated laser beam. Moreover, the use of lasers has been growing more and more in fields such as particle sizing, biomedicine, aerosol cloud penetration, and so on. Hence, for such kind of applications, a shaped beam (Gaussian beam) represents a more realistic incident field. It is worth noting that, despite a Gaussian beam can be represented as a continuous spectrum of plane waves, the analysis of the scattering deserves attention since the convergence of a numerical scheme is strictly related to the functional space to which the free term belongs [6]. On the other hand, the field pattern obtained for a Gaussian beam does not exactly follow the geometrical optics rules of reflection and transmission satisfied by a plane wave [7]. All these reasons have justified the need to address the problem of the scattering of a Gaussian beam from PEC and dielectric objects [8–17].

The aim of this paper is the analysis of the electromagnetic scattering from a PEC polygonal cross-section cylinder when a TM/TE polarized Gaussian beam orthogonally impinges onto the scatterer surface. Since the polygonal cross-section can be reviewed as a collection of strips, integral equation

*Received 7 July 2017, Accepted 18 October 2017, Scheduled 31 October 2017*

* Corresponding author: Mario Lucido (lucido@unicas.it).

The authors are with the D.I.E.I. and ELEDIA Research Center (ELEDIA@UniCAS), Università degli Studi di Cassino e del Lazio Meridionale, Cassino 03043, Italy.

formulations can be obtained by means of the superposition principle. As usual, for TM incidence an electric field integral equation (EFIE) is used, whilst for TE incidence a magnetic field integral equation (MFIE) is preferred. Since no closed form solution is in general available for the problem at hand, numerical methods have to be applied to find an approximation of the exact solution. However, the approximate solutions obtained by discretizing and truncating first-kind or strongly-singular second-kind integral equations cannot converge to the exact solution of the problem. Anyway, due the unboundedness of the involved operator or of its inverse, the sequence of condition numbers diverges. In order to overcome these problems, the Method of analytical preconditioning is applied in this paper [6]. After defining the functional spaces to which the unknown and free term belong, it consists in individuating a suitable expansion basis for the surface current density in a Galerkin scheme such that the most singular part of the integral operator is invertible with a continuous two-side inverse. In this way, the integral equation is recast as a matrix operator equation at which Fredholm theory can be applied [18]. The selected expansion functions have a closed form spectral domain counterpart. This suggests to formulate the problem in the spectral domain so that the convolution integrals can be interpreted as the Fourier transforms in the complex plane of the expansion functions. Moreover, the choice of expansion bases reconstructing the behaviour of the fields on the wedges [19] leads to a fast convergence, i.e., small size of resulting coefficient matrix to achieve highly accurate results. The proposed method is efficient even in terms of computation time since the elements of the coefficient matrix, which are improper integrals of oscillating functions with a slow asymptotic decay in the worst case, are efficiently evaluated by means of an analytical asymptotic acceleration technique. This approach has been successfully applied in propagation, radiation and scattering problems involving PEC/dielectric 2D/3D structures in homogeneous and layered media [20–38].

This paper is organized as follows. Section 2 is devoted to the formulation of the problem while the solution is proposed in Section 3. Numerical results and comparisons with the classical point-matching method (PMM) with piecewise linear basis functions applied to a spatial domain formulation are shown in Section 4 and the conclusions summarized in Section 5.

## 2. FORMULATION OF THE PROBLEM

In Figure 1, the polygonal cross-section of a PEC cylinder is sketched. A coordinate system $(x, y, z)$ is introduced so that the $z$ axis coincides with the cylinder axis. A 2-D aperture antenna is assumed to produce a Gaussian beam independent of the $z$-coordinate variable (hence, the scattered electromagnetic field is in turn invariant along the $z$ axis) impinging onto the scatterer surface with an angle $\phi$ with respect to the $x$ axis. A local coordinate system $(x', y', z)$ is located in the antenna's aperture with the

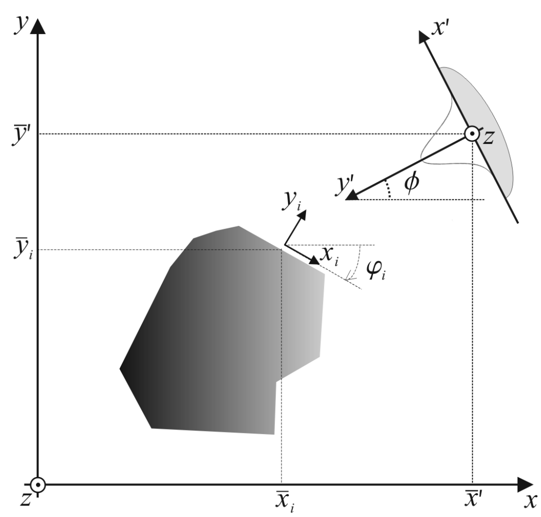


**Figure 1.** Geometry of the problem.

origin at the phase centre of the aperture itself in the position $(\bar{x}', \bar{y}')$. The $L$ sides of the polygonal cross-section can be reviewed as a collection of strips which are conveniently numbered clockwise. On the $i$-th side, a local coordinate system $(x_i, y_i, z)$ is introduced with the origin at the centre of the side itself in position $(\bar{x}_i, \bar{y}_i)$, $\varphi_i$ denotes the orientation of the $x_i$ axis with respect to the $x$ axis and $2a_i$ is the length of the $i$-th side.

### 2.1. Incident Gaussian Beam

For the sake of simplicity, the incident field is assumed to be linearly polarized along the $z$ axis. Let us assume the following Gaussian amplitude distribution in the aperture plane

$$F\left(x', y'\right)\big|_{y'=0} = F_0 e^{-(x'/w_0)^2} \tag{1}$$

where $F \in \{E_z^{inc}, H_z^{inc}\}$, depending on the polarization of the incident field, and $F_0$ is the central amplitude and $w_0$ the beam waist radius.

The incident field can be represented in terms of continuous spectrum of plane waves [8]

$$F\left(x', y'\right) = \int_{-\infty}^{+\infty} \tilde{F}(u) e^{-j(ux' + R(u)y')} du, \tag{2}$$

where

$$R(u) = \begin{cases} \sqrt{k^2 - u^2} & |u| \leq k \\ -j\sqrt{u^2 - k^2} & |u| \geq k \end{cases}, \tag{3}$$

$k = 2\pi/\lambda = \omega\sqrt{\varepsilon\mu}$ is the wavenumber, $\lambda$ the wavelength, $\omega$ the angular frequency, $\varepsilon$ the dielectric permittivity, $\mu$ the magnetic permeability of the medium, and $\tilde{F}(u)$ the Fourier transform of the Gaussian amplitude distribution in the aperture plane with respect to $x'$, i.e.,

$$\tilde{F}(u) = \frac{1}{2\pi} \int_{-\infty}^{+\infty} F\left(x', y'\right)\big|_{y'=0} e^{jux'} dx' = \frac{F_0 w_0}{2\sqrt{\pi}} e^{-(uw_0/2)^2}. \tag{4}$$

It is simple to observe that

$$F\left(\rho', \varphi'\right) \overset{\rho' \to +\infty}{\sim} F_0 w_0 \sin\varphi' \sqrt{\frac{jk}{2\rho'}} e^{-jk\rho'} e^{-(k\cos\varphi' w_0/2)^2} \tag{5}$$

where $x' = \rho'\cos\varphi'$ and $y' = \rho'\sin\varphi'$, i.e., in the far field zone expression (2) can be approximated with a Gaussian beam. Since this paper is aimed at presenting a full-wave approach, the continuous spectrum of plane waves in Eq. (2) will be used as incident field.

By means of the following relations between coordinate systems

$$\begin{cases} x' = -x_i s_i + y_i c_i + \bar{X}_i \\ y' = -x_i c_i - y_i s_i + \bar{Y}_i \end{cases}, \tag{6a}$$

$$s_i = \sin\left(\phi - \varphi_i\right), \tag{6b}$$

$$c_i = \cos\left(\phi - \varphi_i\right), \tag{6c}$$

$$\bar{X}_i = \left(\bar{x}' - \bar{x}_i\right)\sin\phi - \left(\bar{y}' - \bar{y}_i\right)\cos\phi, \tag{6d}$$

$$\bar{Y}_i = \left(\bar{x}' - \bar{x}_i\right)\cos\phi + \left(\bar{y}' - \bar{y}_i\right)\sin\phi, \tag{6e}$$

the incident field on the $i$-th side of the cylinder surface can be simply written as follows

$$F\left(x, y\right)\big|_{y_i=0} = \int_{-\infty}^{+\infty} \tilde{F}(u) e^{-j\left(u\bar{X}_i + R(u)\bar{Y}_i\right)} e^{j(us_i + R(u)c_i)x_i} du. \tag{7}$$

### 2.2. Integral Equation Formulations

The incident field induces a surface current density on each side of the scatterer surface. The potential function generated by the current on the $i$-th side is

$$\underline{A}_i\left(x_i, y_i\right) = \frac{\mu}{4j} \int_{-a_i}^{a_i} \underline{J}_i\left(x_0\right) H_0^{(2)}\left(k\sqrt{\left(x_i - x_0\right)^2 + y_i^2}\right) dx_0 \tag{8}$$

with $i = 1, 2, \ldots, L$, where $\underline{J}_i(\cdot)$ is the surface current density on the $i$-th side, and $H_0^{(2)}(\cdot)$ denotes the Hankel function of second kind and order 0.

Once the physical behaviour of the surface current density is settled, a spectral domain representation of the vector potential can be readily obtained. To this purpose, Meixner's theory [19] allows to state the following behaviour on the wedges

$$J_{iz}\left(x_i\right), \ \frac{\partial}{\partial x_i} J_{ix_i}\left(x_i\right) \underset{x_i \to \pm a_i}{\sim} \left(1 \mp x_i/a_1\right)^{t_i^{\pm}} \tag{9}$$

where $t_i^{\pm} \geq -1/2$. Moreover, the property

$$\lim_{x_i \to a_i} \frac{J_{iz}\left(x_i\right)}{\left(a_i - x_i\right)^{t_i^{+}}} = \lim_{x_{i+1} \to -a_{i+1}} \frac{J_{i+1z}\left(x_{i+1}\right)}{\left(a_{i+1} + x_{i+1}\right)^{t_{i+1}^{-}}}, \tag{10}$$

can be deduced, while the transverse component of the surface current density is continuous even on the wedges.

The asymptotic behaviour of the Fourier transforms of the components of the surface current density with respect to $x_i$ can be established by invoking Watson's lemma [39], i.e.,

$$\tilde{J}_{iz}(u) \overset{|u| \to +\infty}{\sim} \eta_{iz}^{-} \frac{e^{-jua_i}}{u^{t_i^{-}+1}} + \eta_{iz}^{+} \frac{e^{jua_i}}{u^{t_i^{+}+1}}, \tag{11a}$$

$$\tilde{J}_{ix_i}(u) \overset{|u| \to +\infty}{\sim} \frac{\eta_{ix_i}^{+} e^{-jua_i} + \eta_{ix_i}^{-} e^{jua_i}}{2\pi j u}, \tag{11b}$$

where $\eta_{it}^{\pm}$ with $t \in \{x_i, z\}$ are suitable parameters depending on the problem at hand.

Therefore, by means of the superposition principle, the following spectral domain representation for the vector potential can be obtained

$$\underline{A}(x, y) = -j\frac{\mu}{2} \sum_{i=1}^{L} \int_{-\infty}^{+\infty} \underline{\tilde{J}}_i(u) \frac{e^{-j|y_i|R(u)}}{R(u)} e^{-jux_i} du, \tag{12}$$

where the remarkable identity [40]

$$\int_{-\infty}^{+\infty} H_0^{(2)}\left(k\sqrt{\left(x_i - x_0\right)^2 + y_i^2}\right) e^{-jux_0} dx_0 = 2\frac{e^{-j(ux_i + R(u)|y_i|)}}{R(u)} \tag{13}$$

has been used.

For a $z$-directed incident electric field (TM incidence), only TM solutions can be searched for, i.e., the current is directed along the $z$ axis. An EFIE is obtained by imposing the total electric field to be vanishing on the scatterer surface

$$E_z\left(x, y\right)\big|_{|x_j| \leq a_j,\, y_j = 0} = -\left. E_z^{inc}\left(x, y\right)\right|_{|x_j| \leq a_j,\, y_j = 0} \tag{14}$$

with $j = 1, 2, \ldots, L$, where

$$E_z\left(x, y\right) = -j\omega A_z\left(x, y\right) = -\frac{\omega\mu}{2} \sum_{i=1}^{L} \int_{-\infty}^{+\infty} \tilde{J}_{iz}(u) \frac{e^{-j|y_i|R(u)}}{R(u)} e^{-jux_i} du. \tag{15}$$

Analogously, only TE solution (transverse current) can be obtained by means of an incident magnetic field directed along the $z$ axis. An MFIE is obtained by imposing the boundary conditions on the scatterer surface for the magnetic field

$$H_z(x,y)\big|_{|x_j|\le a_j,\, y_j=0} - J_{jx_j}(x_j) = -\, H_z^{inc}(x,\, y)\big|_{|x_j|\le a_j,\, y_j=0} \tag{16}$$

with $j = 1, 2, \dots, L$, where

$$H_z(x,y) = \frac{1}{\mu}\, \nabla\times \underline{A}(x,y)\big|_z = \frac{1}{2}\sum_{i=1}^{L} \operatorname{sgn}(y_i) \int_{-\infty}^{+\infty} \tilde{J}_{ix_i}(u) e^{-j|y_i|R(u)} e^{-jux_i} du, \tag{17}$$

and sgn$(\cdot)$ denotes the signum function.

## 3. METHOD OF ANALYTICAL PRECONDITIONING

A fast converging discretization technique is presented in this section. It consists in the application of Galerkin method with suitable expansion bases chosen in order to reconstruct the behaviour of the surface current density on each side and even on the wedges with closed-form spectral domain counterparts.

The following expansions for the longitudinal and transverse components of the surface current density on the $i$-th side of the cylinder are considered

$$J_{iz}(x_i) \;=\; J_{-1}^{iz}\chi^i\left(\frac{x_h}{a_h}, \frac{x_i}{a_i}\right) + J_{-1}^{jz}\chi^j\left(\frac{x_i}{a_i}, \frac{x_j}{a_j}\right) + \sum_{n=0}^{+\infty} J_n^{iz}\varphi_n^{\left(\bar{t}_i^+, \bar{t}_i^-\right)}\left(\frac{x_i}{a_i}\right), \tag{18a}$$

$$J_{ix_i}(x_i) \;=\; J_{-1}^{ix_i}\bar{\chi}^{ix_i}\left(\frac{x_h}{a_h}, \frac{x_i}{a_i}\right) + J_{-1}^{jx_j}\bar{\chi}^j\left(\frac{x_i}{a_i}, \frac{x_j}{a_j}\right) + \sum_{n=0}^{+\infty} J_n^{ix_i}\varphi_n^{\left(t_i^+ +1, t_i^- +1\right)}\left(\frac{x_i}{a_i}\right), \tag{18b}$$

where $h$, $i$ and $j$ are three consecutive sides,

$$\chi^i\left(\frac{x_h}{a_h}, \frac{x_i}{a_i}\right) = \begin{cases} \dfrac{\varphi_{-1}^{\left(t_h^+, \bar{t}_h^-\right)}(x_h/a_h)}{\sqrt{\left[\xi_{-1}^{\left(t_h^+, \bar{t}_h^-\right)}\right]^2 + \left[\xi_{-1}^{\left(t_i^-, \bar{t}_i^+\right)}\right]^2}} & \text{for } y_h = 0 \\[2ex] \dfrac{\varphi_{-1}^{\left(t_i^-, \bar{t}_i^+\right)}(-x_i/a_i)}{\sqrt{\left[\xi_{-1}^{\left(t_h^+, \bar{t}_h^-\right)}\right]^2 + \left[\xi_{-1}^{\left(t_i^-, \bar{t}_i^+\right)}\right]^2}} & \text{for } y_i = 0 \end{cases}, \tag{19a}$$

$$\bar{\chi}^i\left(\frac{x_h}{a_h}, \frac{x_i}{a_i}\right) = \begin{cases} \dfrac{\bar{\varphi}_{-1}^{\left(t_h^+ +1, t_h^- +1\right)}(x_h/a_h)}{\sqrt{\left[\bar{\xi}_{-1}^{\left(t_h^+ +1, t_h^- +1\right)}\right]^2 + \left[\bar{\xi}_{-1}^{\left(t_i^- +1, t_i^+ +1\right)}\right]^2}} & y_h = 0 \\[2ex] \dfrac{\bar{\varphi}_{-1}^{\left(t_i^- +1, t_i^+ +1\right)}(-x_i/a_i)}{\sqrt{\left[\bar{\xi}_{-1}^{\left(t_h^+ +1, t_h^- +1\right)}\right]^2 + \left[\bar{\xi}_{-1}^{\left(t_i^- +1, t_i^+ +1\right)}\right]^2}} & y_i = 0 \end{cases}, \tag{19b}$$

$$\varphi_{-1}^{(\alpha,\beta)}\left(\frac{x}{a}\right) \;=\; \frac{a^\alpha \xi_0^{(\alpha,\beta)}}{2^\beta}\varphi_0^{(\alpha,\beta)}\left(\frac{x}{a}\right), \tag{19c}$$

$$\bar{\varphi}_{-1}^{(\alpha,\beta)}\left(\frac{x}{a}\right) \;=\; \frac{\mathbf{B}_{(1+x/a)/2}(\beta,\alpha)}{\mathbf{B}(\beta,\alpha)}\Pi\left(\frac{x}{a}\right), \tag{19d}$$

$$\varphi_n^{(\alpha,\beta)}\left(\frac{x}{a}\right) \;=\; \left(1-\frac{x}{a}\right)^\alpha \left(1+\frac{x}{a}\right)^\beta \frac{P_n^{(\alpha,\beta)}(x/a)}{\xi_n^{(\alpha,\beta)}} \prod\left(\frac{x}{a}\right) \tag{19e}$$

with $n = 0, 1, \ldots$,

$$\xi_{-1}^{(\alpha,\beta)} = \sqrt{\int_{-a}^{a} \left(1-\frac{x}{a}\right)^{-\alpha} \left(1+\frac{x}{a}\right)^{-\beta} \left[\varphi_{-1}^{(\alpha,\beta)}\left(\frac{x}{a}\right)\right]^2 dx} = \frac{a^{\alpha}\xi_0^{(\alpha,\beta)}}{2^{\beta}}, \tag{20a}$$

$$\bar{\xi}_{-1}^{(\alpha,\beta)} = \sqrt{\int_{-a}^{a} \left(1+\frac{x}{a}\right)^{-\beta} \left[\varphi_{-1}^{(\alpha,\beta)}\left(\frac{x}{a}\right)\right]^2 dx} = \sqrt{\frac{a2^{1-\beta}}{1-\beta}\left[1-\frac{2}{\alpha}\frac{\mathbf{B}(\beta,2\alpha)}{\mathbf{B}(\beta,\alpha)^2}\right]}, \tag{20b}$$

$$\xi_{n}^{(\alpha,\beta)} = \sqrt{\int_{-a}^{a} \left(1-\frac{x}{a}\right)^{\alpha} \left(1+\frac{x}{a}\right)^{\beta} \left[P_{n}^{(\alpha,\beta)}\left(\frac{x}{a}\right)\right]^2 dx} = \sqrt{\frac{a2^{\alpha+\beta+1}\Gamma(n+\alpha+1)\Gamma(n+\beta+1)}{n!\,(2n+\alpha+\beta+1)\,\Gamma(n+\alpha+\beta+1)}} \tag{20c}$$

where $n = 0, 1, \ldots$ are suitable normalization quantities; $\Pi(\cdot)$ is the unitary rectangular window; $P_n^{(\alpha,\beta)}(\cdot)$ is the Jacobi polynomial of order $n$ with parameters $\alpha$, $\beta$; $\Gamma(\cdot)$ denotes the Gamma function [41], while $B_z(\cdot,\cdot)$ and $B(\cdot,\cdot)$ are the incomplete and complete Beta functions, respectively [41]. The coefficients $\bar{t}_i^{\pm}$ are chosen in order to reconstruct the second order behaviour of the $z$-component of the surface current density on the wedges adjacent to the $i$-th side (the expansion (18a) has been devised so that the first two functions are only responsible for the reconstruction of the first order behaviour of the current on the wedges, while the residual expansion series factorizes the second order edge behaviour of the current itself). Moreover, the property in Eq. (10) and the continuity of the transverse current across the wedges have been imposed.

Galerkin procedure leads to a matrix equation whose elements can be always represented as single integrals. Indeed, by means of algebraic manipulations and the following remarkable identity [40]

$$\int_{-1}^{1} (1-x)^{\nu-1}(1+x)^{\mu-1} e^{-jux} dx = 2^{\mu+\nu+1}\mathbf{B}(\mu,\nu)\, e^{ju}\, {}_1F_1(\mu;\mu+\nu;-2ju), \tag{21}$$

where ${}_1F_1(\cdot\,;\,\cdot\,;\,\cdot)$ is the confluent hypergeometric function of first kind [41], the Fourier transforms of the expansion functions in Eqs. (19c), (19d) and (19e) can be expressed in closed-form. Moreover, by means of reciprocity, it is simple to individuate a representation of the matrix coefficients such that the convolution integrals can be always interpreted as the Fourier transforms in the complex plane of the expansion functions, i.e., they can be always reduced to algebraic products. To conclude, the matrix coefficients are single improper integrals involving products of confluent hypergeometric functions of the first kind, which, in the worst case, are efficiently evaluated by means of an analytical asymptotic acceleration technique consisting of the extraction from the kernels of their asymptotic behaviour, while the slowly converging integrals of the extracted parts are expressed in closed form.

Even the free term elements can be reduced to single integrals of the kind

$$\int_{-\infty}^{+\infty} \tilde{F}(u) e^{-j\left(u\bar{X}_j + R(u)\bar{Y}_j\right)} \tilde{\varphi}_m^{(\alpha_j,\beta_j)}\left(a_j\left(us_j + R(u)c_j\right)\right) du \tag{22}$$

with $m = 0, 1, \ldots$ and $j = 1, 2, \ldots, L$, where $\tilde{\varphi}_m^{(\alpha,\beta)}(\cdot)$ denotes the Fourier transform of the general expansion function. Due to the exponential decay of $\tilde{F}(\cdot)$, the convergence of the integral in Eq. (22) is very fast. On the other hand, the incident field is a regular function on the scatterer surface since originating from a sources off the surface itself, i.e., it can be quickly reconstructed by means of a uniformly converging series of polynomial. As a consequence, the sequence of free term elements decreases very quickly (exponential decaying), and the analytical regularizing procedure first developed in [21] for an impinging plane wave can be readily generalized to the case at hand.

## 4. NUMERICAL RESULTS

In this section, the fast convergence of the presented method in terms of computation time and storage requirements will be shown.

To this purpose, the following normalized truncation error is introduced

$$\mathrm{err}(N) = \|\mathbf{J}_{N+1} - \mathbf{J}_N\| / \|\mathbf{J}_N\|, \tag{23}$$

where $\|\cdot\|$ is the usual Euclidean norm, and $\mathbf{J}_M$ is the vector of all the expansion coefficients of the currents on all the sides evaluated with $M$ terms on each side.

In Figure 2, the normalized truncation error for the scatterer sketched in the inset with $\overline{\mathrm{AB}} = a/2$, $\overline{\mathrm{BC}} = a/4$, $\overline{\mathrm{CD}} = a\sqrt{5+2\sqrt{2}}/4$, $\overline{\mathrm{DA}} = a/\sqrt{2}$, $\mathrm{B\hat{A}D} = \pi/4$, $\mathrm{C\hat{B}A} = 3\pi/4$, $\mathrm{D\hat{C}B} = \pi/4 - \arctan(1/(2\sqrt{2}+1))$, $\mathrm{C\hat{D}A} = \pi/4 + \arctan(1/(2\sqrt{2}+1))$ is plotted for $a = \lambda, 2\lambda, 4\lambda, 8\lambda$ as a function of the number of expansion functions $N$ used on each of the $L$ sides of the polygonal cross-section. An aperture antenna, with phase centre at a distance $\rho = 50\lambda$ from the midpoint of the side $\overline{\mathrm{AB}}$, generates a TM/TE polarized Gaussian beam with waist radius $w_0 = 5\lambda$ impinging onto the scatterer surface with an angle $\phi = \pi/2$. As can be seen, after considering a reasonable number of expansion functions, depending on the size of the cylinder, needed to accurately reconstruct the compact part of the discretized operator, the convergence becomes very fast in all the examined cases. Consequently, highly accurate results are obtained by using few expansion functions. As an example, a normalized truncation error less than

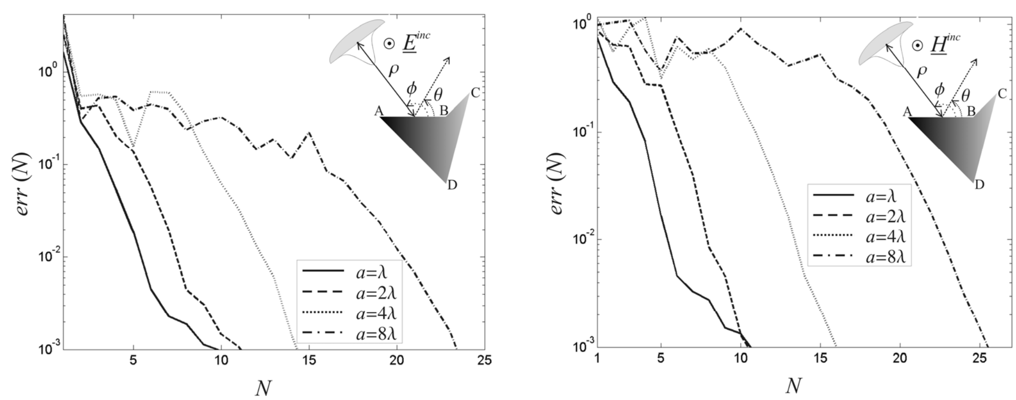


(a) (b)

**Figure 2.** Normalized truncation error for the geometry sketched in the inset and different sides length when a (a) TM and (b) TE polarized Gaussian beam impinges onto the scatterer surface. $\overline{\mathrm{AB}} = a/2$, $\overline{\mathrm{BC}} = a/4$, $\overline{\mathrm{CD}} = a\sqrt{5+2\sqrt{2}}/4$, $\overline{\mathrm{DA}} = a/\sqrt{2}$, $\mathrm{B\hat{A}D} = \pi/4$, $\mathrm{C\hat{B}A} = 3\pi/4$, $\mathrm{D\hat{C}B} = \pi/4 - \arctan(1/(2\sqrt{2}+1))$, $\mathrm{C\hat{D}A} = \pi/4 + \arctan(1/(2\sqrt{2}+1))$, $w_0 = 5\lambda$, $\rho = 50\lambda$, $\phi = \pi/2$.

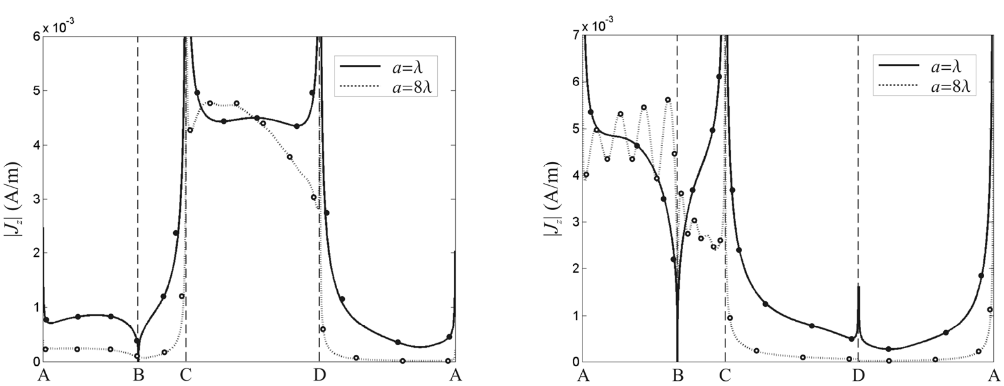


(a) (b)

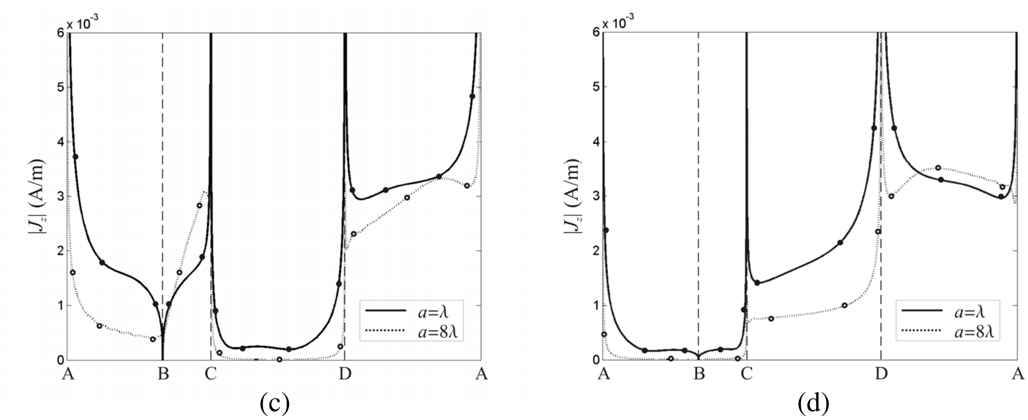


**Figure 3.** Surface current density for the geometry sketched in the inset of Figure 2(a) and different sides length when a TM polarized Gaussian beam impinges onto the scatterer surface with an angle (a) $\phi = 0$, (b) $\phi = \pi/2$, (c) $\phi = \pi$ and (d) $\phi = 3\pi/2$. $\overline{\mathrm{AB}} = a/2$, $\overline{\mathrm{BC}} = a/4$, $\overline{\mathrm{CD}} = a\sqrt{5+2\sqrt{2}}/4$, $\overline{\mathrm{DA}} = a/\sqrt{2}$, $\mathrm{B\hat{A}D} = \pi/4$, $\mathrm{C\hat{B}A} = 3\pi/4$, $\mathrm{D\hat{C}B} = \pi/4 - \arctan(1/(2\sqrt{2}+1))$, $\mathrm{C\hat{D}A} = \pi/4 + \arctan(1/(2\sqrt{2}+1))$, $w_0 = 5\lambda$, $\rho = 50\lambda$, $|E_z| = 1\,\mathrm{V/m}$. Lines: this method; circles: PMM.

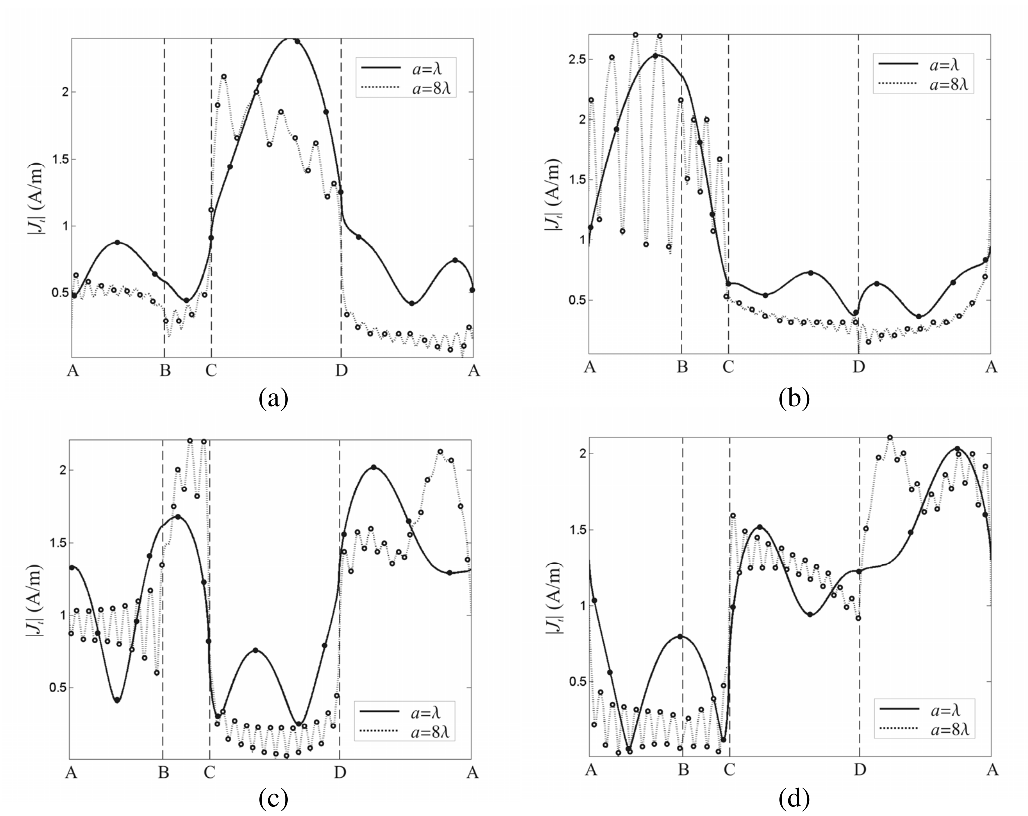


**Figure 4.** Surface current density for the geometry sketched in the inset of Figure 2(b) and different sides length when a TE polarized Gaussian beam impinges onto the scatterer surface with an angle (a) $\phi = 0$, (b) $\phi = \pi/2$, (c) $\phi = \pi$ and (d) $\phi = 3\pi/2$. $\overline{\mathrm{AB}} = a/2$, $\overline{\mathrm{BC}} = a/4$, $\overline{\mathrm{CD}} = a\sqrt{5+2\sqrt{2}}/4$, $\overline{\mathrm{DA}} = a/\sqrt{2}$, $\mathrm{B\hat{A}D} = \pi/4$, $\mathrm{C\hat{B}A} = 3\pi/4$, $\mathrm{D\hat{C}B} = \pi/4 - \arctan(1/(2\sqrt{2}+1))$, $\mathrm{C\hat{D}A} = \pi/4 + \arctan(1/(2\sqrt{2}+1))$, $w_0 = 5\lambda$, $\rho = 50\lambda$, $|H_z| = 1\,\mathrm{A/m}$. Lines: this method; circles: PMM.

$10^{-1}, 10^{-2}, 10^{-3}$ is achieved by using a number of expansion functions on each side ranging from 3, 6, 10 to 19, 23, 26, respectively. On the other hand, more that 25 integrals per second are evaluated on a laptop equipped with an Intel Core 2 Duo CPU T9600 2.8 GHz, 3 GB RAM, running Windows XP by means

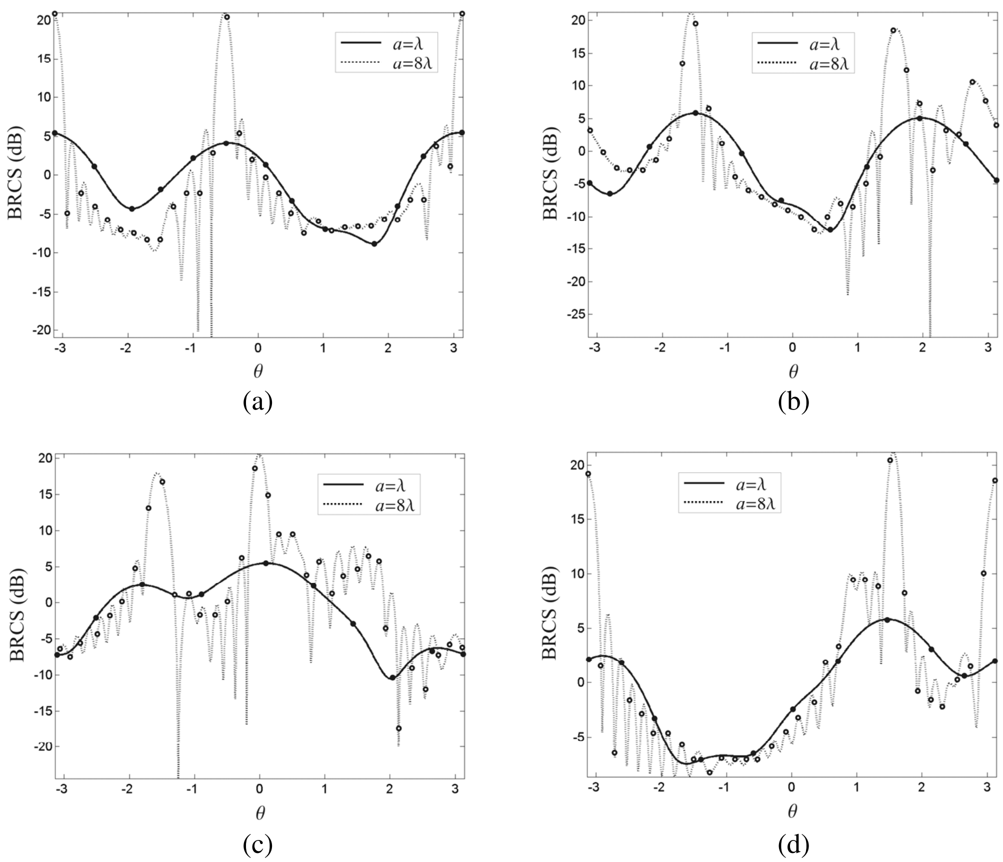


**Figure 5.** Bistatic radar cross section for the geometry sketched in the inset of Figure 2(a) and different sides length when a TM polarized Gaussian beam impinges onto the scatterer surface with an angle (a) $\phi = 0$, (b) $\phi = \pi/2$, (c) $\phi = \pi$ and (d) $\phi = 3\pi/2$. $\overline{\mathrm{AB}} = a/2$, $\overline{\mathrm{BC}} = a/4$, $\overline{\mathrm{CD}} = a\sqrt{5+2\sqrt{2}}/4$, $\overline{\mathrm{DA}} = a/\sqrt{2}$, $\mathrm{B\hat{A}D} = \pi/4$, $\mathrm{C\hat{B}A} = 3\pi/4$, $\mathrm{D\hat{C}B} = \pi/4 - \arctan(1/(2\sqrt{2}+1))$, $\mathrm{C\hat{D}A} = \pi/4 + \arctan(1/(2\sqrt{2}+1))$, $w_0 = 5\lambda$, $\rho = 50\lambda$, $|E_z| = 1\,\mathrm{V/m}$. Lines: this method; circles: PMM.

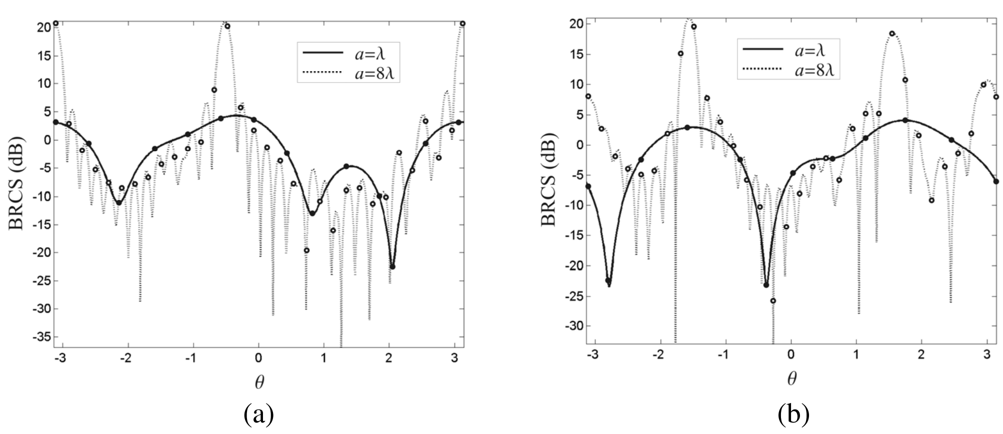

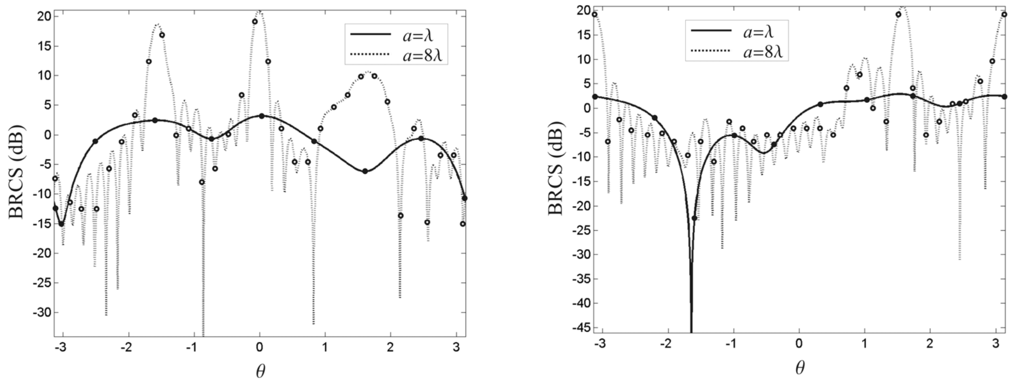


(c) (d)

**Figure 6.** Bistatic radar cross section for the geometry sketched in the inset of Figure 2(b) and different sides length when a TE polarized Gaussian beam impinges onto the scatterer surface with an angle (a) $\phi = 0$, (b) $\phi = \pi/2$, (c) $\phi = \pi$ and (d) $\phi = 3\pi/2$. $\overline{\mathrm{AB}} = a/2$, $\overline{\mathrm{BC}} = a/4$, $\overline{\mathrm{CD}} = a\sqrt{5+2\sqrt{2}}/4$, $\overline{\mathrm{DA}} = a/\sqrt{2}$, $\mathrm{B\hat{A}D} = \pi/4$, $\mathrm{C\hat{B}A} = 3\pi/4$, $\mathrm{D\hat{C}B} = \pi/4 - \arctan(1/(2\sqrt{2}+1))$, $\mathrm{C\hat{D}A} = \pi/4 + \arctan(1/(2\sqrt{2}+1))$, $w_0 = 5\lambda$, $\rho = 50\lambda$, $|H_z| = 1\,\mathrm{A/m}$. Lines: this method; circles: PMM.

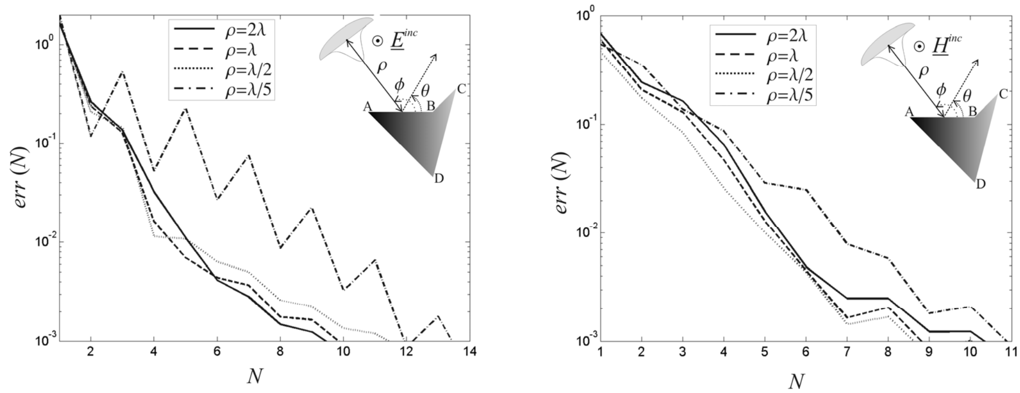


(a) (b)

**Figure 7.** Normalized truncation error for the geometry sketched in the inset and different distances of the aperture antenna from the cylinder surface when a (a) TM and (b) TE polarized Gaussian beam impinges onto the scatterer surface. $a = \lambda$, $\overline{\mathrm{AB}} = a/2$, $\overline{\mathrm{BC}} = a/4$, $\overline{\mathrm{CD}} = a\sqrt{5+2\sqrt{2}}/4$, $\overline{\mathrm{DA}} = a/\sqrt{2}$, $\mathrm{B\hat{A}D} = \pi/4$, $\mathrm{C\hat{B}A} = 3\pi/4$, $\mathrm{D\hat{C}B} = \pi/4 - \arctan(1/(2\sqrt{2}+1))$, $\mathrm{C\hat{D}A} = \pi/4 + \arctan(1/(2\sqrt{2}+1))$, $w_0 = \lambda/100$, $\phi = 50\pi/2$.

of an adaptive Gaussian quadrature routine. Since $N^2L^2$ integrals have to be numerically evaluated in the TE case while they can be reduced to $NL(NL+1)/2$ in the TM case due to reciprocity, it is not difficult to understand that highly accurate results can be obtained very quickly (with a computation of at most few minutes).

For the sake of completeness, the components of the surface current density and the bistatic radar cross section (BRCS) for the same geometry and incident field of the previous example when $\phi = 0, \pi/2, \pi, 3\pi/2$ and $a = \lambda, 8\lambda$ are sketched in Figures 3, 4 and 5, 6, respectively. In order to validate the obtained numerical results, comparisons with the PMM with piecewise linear basis functions applied to a spatial domain formulation are provided showing a very good agreement. It is worth noting that such a method requires in the worst case 1000 expansion functions and a computation time of about 30

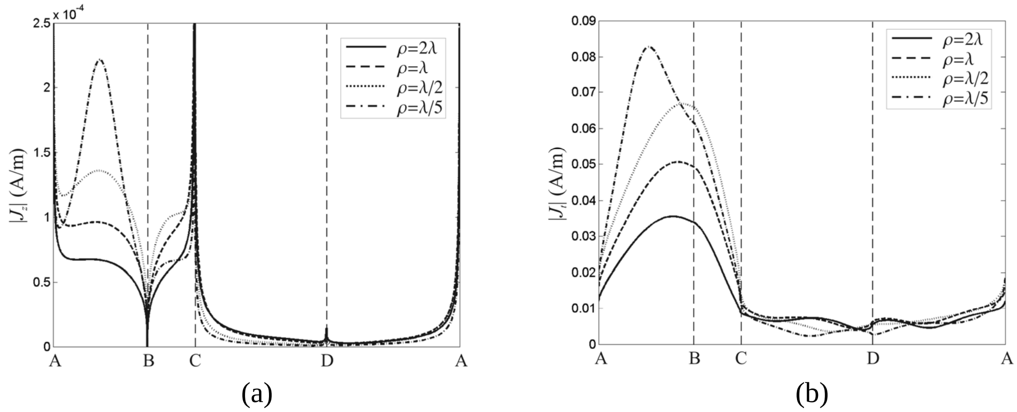


**Figure 8.** Surface current density for the geometry sketched in the inset of Figure 7 and different distances of the aperture antenna from the cylinder surface when a (a) TM and (b) TE polarized Gaussian beam impinges onto the scatterer surface. $a = \lambda$, $\overline{\mathrm{AB}} = a/2$, $\overline{\mathrm{BC}} = a/4$, $\overline{\mathrm{CD}} = a\sqrt{5+2\sqrt{2}}/4$, $\overline{\mathrm{DA}} = a/\sqrt{2}$, $\mathrm{B\hat{A}D} = \pi/4$, $\mathrm{C\hat{B}A} = 3\pi/4$, $\mathrm{D\hat{C}B} = \pi/4 - \arctan(1/(2\sqrt{2}+1))$, $\mathrm{C\hat{D}A} = \pi/4 + \arctan(1/(2\sqrt{2}+1))$, $w_0 = \lambda/100$, $\phi = 50\pi/2$, (a) $|E_z| = 1\,\mathrm{V/m}$ and (b) $|H_z| = 1\,\mathrm{A/m}$.

minutes in order to obtain a reasonable reconstruction of the behaviour of the surface current even on the wedges.

The last example is aimed at showing the effectiveness of the proposed method even when the waist radius is very small with respect to the cylinder cross-section, for different distances of the aperture antenna from the cylinder surface. In Figures 7 and 8, the normalized truncation error and the surface current density for the same scatterer of the previous examples with $a = \lambda$, when an aperture antenna, with phase centre at distances $\rho = \lambda/5, \lambda/2, \lambda, 2\lambda$ from the midpoint of the side $\overline{\mathrm{AB}}$ generates a TM/TE polarized Gaussian beam with waist radius $w_0 = \lambda/100$ impinging onto the scatterer surface with an angle $\phi = \pi/2$, are, respectively, sketched. As can be seen, the convergence is very good even when the aperture antenna is close to the scatterer surface.

## 5. CONCLUSIONS

In this paper, the analysis of the electromagnetic scattering from PEC polygonal cross-section cylinders when a Gaussian beam impinges upon it has been addressed by means of a very effective method. As clearly shown in the Numerical Results section, fast convergence is achieved in terms of both computation time and storage requirements. Future perspective is the extension of the method to problems in which both dielectric and conducting cylinders are involved.

## REFERENCES


1. Harrington, R. F., *Field Computation by Moment Methods*, Macmillan, New York, 1968.
2. Roy, T., T. K. Sarkar, A. R. Djordjevic, and M. Salazar-Palma, "A hybrid method solution of scattering by conducting cylinders (TM case)," *IEEE Trans. Microw. Theory Tech.*, Vol. 44, No. 12, 2145–2151, Dec. 1996.
3. Yashiro, K. and S. Ohkawa, "Boundary element method for electromagnetic scattering from cylinders," *IEEE Trans. Antennas Propag.*, Vol. 33, No. 4, 383–389, Apr. 1985.
4. Michaeli, A., "A uniform GTD solution for the far-field scattering by polygonal cylinders and strips," *IEEE Trans. Antennas Propag.*, Vol. 35, No. 8, 983–986, Aug. 1987.
5. Tiberio, R., G. Manara, G. Pelosi, and R. G. Kouyoumijian, "High frequency electromagnetic scattering of plane waves from double wedges," *IEEE Trans. Antennas Propag.*, Vol. 37, No. 9, 1172–1180, Sep. 1989.

6. Nosich, A. I., "Method of analytical regularization in computational photonics," *Radio Science*, Vol. 51, No. 8, 1421–1430, Aug. 2016.
7. Li, Q. and R. J. Vernon, "Theoretical and experimental investigation of Gaussian beam transmission and reflection by a dielectric slab at 110 GHz," *IEEE Trans. Antennas Propag.*, Vol. 54, No. 11, 3449–3457, Nov. 2006.
8. Collin, R. E., "Scattering of an incident gaussian beam by a perfectly conducting rough surface," *IEEE Trans. Antennas Propag.*, Vol. 42, No. 1, 70–74, Jan. 1994.
9. Shavit, R., T. Wells, and A. Cohen, "Scattering analysis of arbitrarily shaped cylinders in a focused beam system," *IEE Proc. — Microw. Antennas Propag.*, Vol. 145, No. 4, 289–294, Aug. 1998.
10. Pelosi, G. and S. Selleri, "A numerical approach for the diffraction of a Gaussian beam from a perfectly conducting wedge," *IEEE Trans. Antennas Propag.*, Vol. 47, No. 10, 1555–1559, Oct. 1999.
11. Petersson, L. E. R. and G. S. Smith, "Three-dimensional electromagnetic diffraction of a Gaussian beam by a perfectly conducting half-plane," *J. Opt. Soc. Am. A*, Vol. 19, No. 11, 2265–2280, Nov. 2002.
12. Wang, G. X., Y.-B. Gan, and L.-W. Li, "Electromagnetic scattering by partially buried PEC cylinder at the dielectric rough surface interface: TM case," *IEEE Antennas and Wireless Propagation Letters*, Vol. 2, 319–322, 2003.
13. Yang, J., L.-W. Li, K. Yasumoto, and C.-H. Liang, "Two-dimensional scattering of a Gaussian beam by a periodic array of circular cylinders," *IEEE Trans. on Geoscience and Remote Sensing*, Vol. 43, No. 2, 280–285, Feb. 2005.
14. Hillairet, J., J. Sokoloff, and S. Bolioli, "Uniform analytic scattered fields of a PEC plate illuminated by a vector paraxial gaussian beam," *Progress In Electromagnetic Research B*, Vol. 14, 203–217, 2009.
15. Zhang, H., Y. Sun, and Z. Huang, "Scattering by a multilayered infinite cylinder arbitrarily illuminated with a shaped beam," *IEEE Trans. Antennas Propag.*, Vol. 59, No. 11, 4369–4371, Nov. 2011.
16. Han, Y., Z. Cui, and W. Zhao, "Scattering of Gaussian beam by arbitrarily shaped particles with multiple internal inclusions," *Opt. Express*, Vol. 20, 718–731, 2012.
17. Whitman, G. M., Q. Wang, P. Spector, and F. K. Schwering, "Gaussian beam scattering from a deterministic rough metal surface," *IEEE Trans. Antennas Propag.*, Vol. 64, No. 5, 1868–1876, May 2016.
18. Kolmogorov, A. N. and S. V. Fomin, *Elements of the Theory of Functions and Functional Analysis*, Dover, New York, 1999.
19. Meixner, J., "The behavior of electromagnetic fields at edges," *IEEE Trans. Antennas Propag.*, Vol. 20, 442–446, 1972.
20. Eswaran, K., "On the solutions of a class of dual integral equations occurring in diffraction problems," *Proc. Roy. Soc. London*, Ser. A, Vol. 429, 399–427, 1990.
21. Veliev, E. I. and V. V. Veremey, "Numerical-analytical approach for the solution to the wave scattering by polygonal cylinders and flat strip structures," *Analytical and Numerical Methods in Electromagnetic Wave Theory*, M. Hashimoto, M. Idemen, and O. A. Tretyakov (eds.), Science House, Tokyo, 1993.
22. Davis, M. J. and R. W. Scharstein, "Electromagnetic plane wave excitation of an open-ended finite-length conducting cylinder," *Journal of Electromagnetic Waves and Applications*, Vol. 7, 301–319, 1993.
23. Hongo, K. and H. Serizawa, "Diffraction of electromagnetic plane wave by rectangular plate and rectangular hole in the conducting plate," *IEEE Trans. Antennas Propag.*, Vol. 47, No. 6, 1029–1041, Jun. 1999.
24. Bliznyuk, N. Y., A. I. Nosich, and A. N. Khizhnyak, "Accurate computation of a circular-disk printed antenna axisymmetrically excited by an electric dipole," *Microwave and Optical Technology Letters*, Vol. 25, No. 3, 211–216, 2000.

25. Tsalamengas, J. L., "Rapidly converging direct singular integral-equation techniques in the analysis of open microstrip lines on layered substrates," *IEEE Trans. Microw. Theory Tech.*, Vol. 49, No. 3, 555–559, Mar. 2001.
26. Losada, V., R. R. Boix, and F. Medina, "Fast and accurate algorithm for the short-pulse electromagnetic scattering from conducting circular plates buried inside a lossy dispersive half-space," *IEEE Trans. Geosci. Remote Sensing*, Vol. 41, 988–997, May 2003.
27. Lucido, M., G. Panariello, and F. Schettino, "Accurate and efficient analysis of stripline structures," *Microwave and Optical Technology Letters*, Vol. 43, No. 1, 14–21, Oct. 2004.
28. Hongo, K. and Q. A. Naqvi, "Diffraction of electromagnetic wave by disk and circular hole in a perfectly conducting plane," *Progress In Electromagnetics Research*, Vol. 68, 113–150, 2007.
29. Coluccini, G., M. Lucido, and G. Panariello, "TM scattering by perfectly conducting polygonal cross-section cylinders: A new surface current density expansion retaining up to the second-order edge behavior," *IEEE Trans. Antennas Propag.*, Vol. 60, No. 1, 407–412, Jan. 2012.
30. Lucido, M., "An analytical technique to fast evaluate mutual coupling integrals in spectral domain analysis of multilayered coplanar coupled striplines," *Microwave and Optical Technology Letters*, Vol. 54, No. 4, 1035–1039, Apr. 2012.
31. Coluccini, G., M. Lucido, and G. Panariello, "Spectral domain analysis of open single and coupled microstrip lines with polygonal cross-section in bound and leaky regimes," *IEEE Trans. Microw. Theory Tech.*, Vol. 61, No. 2, 736–745, Feb. 2013.
32. Lucido, M., "An efficient evaluation of the self-contribution integrals in the spectral-domain analysis of multilayered striplines," *IEEE Antennas and Wireless Propagation Letters*, Vol. 12, 360–363, 2013.
33. Coluccini, G. and M. Lucido, "A new high efficient analysis of the scattering by a perfectly conducting rectangular plate," *IEEE Trans. Antennas Propag.*, Vol. 61, No. 5, 2615–2622, May 2013.
34. Lucido, M., "Electromagnetic scattering by a perfectly conducting rectangular plate buried in a lossy half-space," *IEEE Trans. Geosci. Remote Sensing*, Vol. 52, No. 10, 6368–6378, Oct. 2014.
35. Corsetti, F., M. Lucido, and G. Panariello, "Effective analysis of the propagation in coupled rectangular-core waveguides," *IEEE Photonics Technology Letters*, Vol. 26, No. 18, 1855–1858, Sep. 2014.
36. Di Murro, F., M. Lucido, G. Panariello, and F. Schettino, "Guaranteed-convergence method of analysis of the scattering by an arbitrarily oriented zero-thickness PEC disk buried in a lossy half-space," *IEEE Trans. Antennas Propag.*, Vol. 63, No. 8, 3610–3620, Aug. 2015.
37. Lucido, M., M. D. Migliore, and D. Pinchera, "A new analytically regularizing method for the analysis of the scattering by a hollow finite-length PEC circular cylinder," *Progress In Electromagnetics Research B*, Vol. 70, 55–71, 2016.
38. Lucido, M., G. Panariello, and F. Schettino, "Scattering by a zero-thickness PEC disk: A new analytically regularizing procedure based on Helmholtz decomposition and galerkin method," *Radio Science*, Vol. 52, No. 1, 2–14, Jan. 2017.
39. Jones, D. S., *The Theory of Electromagnetism*, Pergamon Press, 1964.
40. Gradshteyn, I. S. and I. M. Ryzhik, *Table of Integrals, Series, and Products*, Academic, London, U.K., 1994.
41. Abramowitz, M. and I. A. Stegun, *Handbook of Mathematical Functions*, Verlag Harri Deutsch, The Netherlands, 1984.